JOURNAL OF VIROLOGY, Aug. 2009, p. 8141–8152 Vol. 83, No. 16
0022-538X/09/$08.00+0 doi:10.1128/JVI.02116-08

Activation of Intracellular Signaling Pathways by the Murine Cytomegalovirus G Protein-Coupled Receptor M33 Occurs via PLC-β/PKC-Dependent and -Independent Mechanisms▽†

Joseph D. Sherrill, Melissa P. Stropes, Olivia D. Schneider, Diana E. Koch, Fabiola M. Bittencourt, Jeanette L. C. Miller, and William E. Miller*

Department of Molecular Genetics, Biochemistry, and Microbiology, University of Cincinnati College of Medicine, Cincinnati, Ohio 45267-0524

Received 7 October 2008/Accepted 22 May 2009

The presence of numerous G protein-coupled receptor (GPCR) homologs within the herpesvirus genomes suggests an essential role for these genes in viral replication in the infected host. Such is the case for murine cytomegalovirus (MCMV), where deletion of the M33 GPCR or replacement of M33 with a signaling defective mutant has been shown to severely attenuate replication in vivo. In the present study we utilized a genetically altered version of M33 (termed R131A) in combination with pharmacological inhibitors to further characterize the mechanisms by which M33 activates downstream signaling pathways. This R131A mutant of M33 fails to support salivary gland replication in vivo and, as such, is an important tool that can be used to examine the signaling activities of M33. We show that M33 stimulates the transcription factor CREB via heterotrimeric $G_{q/11}$ proteins and not through promiscuous coupling of M33 to the G_s pathway. Using inhibitors of signaling molecules downstream of $G_{q/11}$, we demonstrate that M33 stimulates CREB transcriptional activity in a phospholipase C-β and protein kinase C (PKC)-dependent manner. Finally, utilizing wild-type and R131A versions of M33, we show that M33-mediated activation of other signaling nodes, including the mitogen-activated protein kinase family member p38α and transcription factor NF-κB, occurs in the absence of $G_{q/11}$ and PKC signaling. The results from the present study indicate that M33 utilizes multiple mechanisms to modulate intracellular signaling cascades and suggest that signaling through PLC-β and PKC plays a central role in MCMV pathogenesis in vivo.

Cytomegaloviruses (CMVs) are members of the betaherpesvirus family and are characterized by strict species specificity, a slow replication cycle, and the ability to establish a lifelong persistent infection within the infected host. While present within ~50 to 90% of the world's adult population with little clinical evidence of infection, the human cytomegalovirus (HCMV) is an important pathogen within immunocompromised hosts (39). For instance, HCMV is a common cause of congenital birth defects, including vision and hearing loss, encephalitis, and mental retardation (8). Transplant rejection and increased morbidity in organ transplant recipients and human immunodeficiency virus (HIV)/AIDS patients, respectively, have also been linked to HCMV infection (38, 69). However, the species specificity of HCMV prevents in vivo analysis of HCMV infection and thus hampers the identification of many important pathogenic factors. Murine CMV (MCMV) has been used extensively as a model virus for analyzing HCMV-host interactions due to its similarities to HCMV in genetic makeup and disease progression (42). Primary MCMV infection induces organ-specific immune responses from NK cells and T lymphocytes that promote clearance of the virus from liver and spleen by 7 days postinfection (10, 11, 36, 37). Salivary glands, however, can remain MCMV-positive for up to 6 weeks after infection and thus serve as sites of CMV persistence within the host (46). Consequently, the salivary glands present a major route for horizontal CMV transmission through prolonged viral shedding within saliva secretions.

Molecular mimicry, i.e., the expression of viral proteins with similar structure and/or function as cellular proteins, is a strategy used by CMV and other viruses to alter normal cellular processes in an effort to evade detection by the host immune system allowing for efficient replication in many tissues. Interestingly, several members of the *Herpesviridae* family encode homologs of cellular G protein-coupled receptors (GPCRs) (65). Members of this large and diverse GPCR superfamily can activate intracellular signaling cascades by catalyzing the exchange of GDP for GTP on the Gα subunit of heterotrimeric G protein complexes (59). The activated GTP-bound Gα subunit then alters the enzymatic activity of target effector proteins, which in turn generate downstream second messengers to stimulate cellular responses. For example, activation of the G_s family of heterotrimeric G proteins stimulates adenylate cyclase, leading to cyclic AMP production and the activation of protein kinase A (PKA) (59). Signaling through the $G_{q/11}$ family enhances phospholipase C β (PLC-β) activity, leading to the

* Corresponding author. Mailing address: Department of Molecular Genetics, Biochemistry, and Microbiology, University of Cincinnati College of Medicine, 231 Albert Sabin Way, Cincinnati, OH 45267-0524. Phone: (513) 558-0866. Fax: (513) 558-8474. E-mail: william.miller@uc.edu.

† Supplemental material for this article may be found at http://jvi.asm.org/.

▽ Published ahead of print on 3 June 2009.

generation of inositol 1,4,5-triphosphate (IP_3) and diacylglcerol (DAG) (59). The accumulation of IP_3 causes release of intracellular Ca^{2+} that, in concert with DAG, activates PKC family members. Recent evidence from several groups has demonstrated that GPCRs can also activate downstream signaling events utilizing a mechanism(s) independent of strictly G protein coupling (1, 3, 26, 47). It has been demonstrated that the herpesvirval GPCRs can activate a similar set of these cellular signaling pathways (65). Moreover, it has been shown that these virally encoded GPCRs are functionally important in vivo in animal models of herpesvirus infection (5, 6, 21, 45, 56).

MCMV and HCMV share a large number of conserved genes arranged within a similar genomic architecture. MCMV encodes the GPCR homolog M33, which is highly conserved among MCMV isolates and exhibits ca. 47% nucleotide sequence identity with the HCMV GPCR homolog UL33 (21, 67). However, from a functional perspective M33 possesses similar signaling activities to another HCMV-encoded GPCR termed US28 (66, 75). Both M33 and US28 have been shown to activate heterotrimeric $G_{q/11}$ proteins, leading to increased PLC-β activity (16, 66, 70). In addition, these viral receptors can enhance CREB and NF-κB transcriptional activities (75). In the case of US28, CREB activation is attenuated in the presence of both PLC-β and broad-spectrum PKC inhibitors, suggesting a role for US28 coupling to the $G_{q/11}$ pathway to promote CREB activation (48). UL33 also stimulates CREB activation, however, in contrast to US28, this activity appears to be mediated via UL33 coupling to the G_s pathway and not the $G_{q/11}$ pathway (17). The exact mechanism for M33 activation of CREB and whether this involves the coupling of M33 to G_s or $G_{q/11}$ proteins remains unknown.

Although dispensable for viral replication in cell culture, M33 has been shown to play an essential role in the MCMV life cycle in vivo, since it is necessary for MCMV replication in sites of persistence such as the salivary glands and is important in the regulation of latency (14, 21). Recent work from the same group showed that this effect was dependent on M33 signaling activity, since a recombinant MCMV expressing an M33 mutant containing a point mutation within a conserved GPCR signaling motif, M33(R131Q) failed to replicate within the salivary glands (18). This conserved motif, termed the DRY motif, is an Asp-Arg-Tyr (DRY) sequence in most cellular GPCRs and an Asn-Arg-Tyr (NRY) sequence in M33. The DRY motif has been extensively studied on both a biochemical and functional level for many cellular receptors (2, 12, 44). It is postulated that the residues of the DRY motif provide important structural interactions that are necessary for the receptor to maintain a defined conformational state, active versus inactive, in the presence or absence of agonist, respectively (25). Studies show that, depending on the type of GPCR, replacement of different residues within the DRY motif can have various effects on G protein signaling from imparting constitutive or agonist-independent G protein activation to complete ablation of G protein signaling (25).

In the present study we examine the mechanism(s) by which M33 promotes signal transduction leading to activation of CREB, p38 mitogen-activated protein kinase (MAPK), and NF-κB. The data indicate that M33 utilizes multiple mechanisms to activate downstream signaling pathways and that these pathways bifurcate at the level of the receptor/G-protein interaction. Taken together, our data suggest that M33-directed activation of p38 and/or NF-κB is not sufficient to support viral replication within the salivary gland and that M33 activation of PLC-β, PKC, and CREB may play an important role in MCMV replication in vivo.

MATERIALS AND METHODS

Reagents. Anisomycin, BAPTA-AM, isoproterenol, and the PKA inhibitor H-89 were purchased from Sigma-Aldrich. *Trans*IT-LT1 transfection reagent was purchased from Mirus Bio Corp. and used according to the manufacturer's protocol. The IP_3 receptor inhibitor 2-aminoethoxydiphenyl borate (2-APB), the diacylglycerol (DAG) kinase inhibitor II (R59949) and the PKC inhibitors Ro-32-0432, Bisindoylmaleimide I, and Gö6976 were purchased from Calbiochem. The phospholipase C inhibitor U-73122 was purchased from Cayman Chemical. All inhibitors were used at concentrations similar to those reported in the literature.

Plasmids. Cloning of M33FLAG(WT) and M33FLAG(R131A) into pcDNA3 (Invitrogen) has been described (66). The luciferase reporter plasmid pFR-Luc and the CREB fusion transactivator plasmid pFA2-CREB were purchased from Stratagene. The NF-κB luciferase reporter plasmid 3X-MHC-Luc contains three NF-κB binding sites from the major histocompatibility complex I enhancer driving luciferase expression and was provided by Albert S. Baldwin, Jr. (University of North Carolina School of Medicine, Chapel Hill). The *Renilla* luciferase plasmid pRL-CMV was purchased from Promega. pcDNA3 FLAG-p38α was provided by Roger J. Davis (University of Massachusetts Medical School, Worcester), and the pCMV FLAG-VASP construct was provided by Michael Uhler (University of Michigan, Ann Arbor). The RH domain of GRK2 (amino acids 1 to 190) was cloned from pcDNA3 mycGRK2 (66) and inserted into the HindIII and XbaI sites of pcDNA3.

Cell lines. Human embryonic kidney cells (HEK293) were purchased from the ATCC (CRL-1573) and maintained at 37°C in 5% CO_2 in minimal essential medium supplemented with 10% FetalClone III (HyClone) and penicillin-streptomycin. NIH 3T3 cells (CRL-1658) were purchased from the American Type Culture Collection and maintained at 37°C in 5% CO_2 in Dulbecco modified essential medium supplemented with 2 mM L-glutamine, 10% FetalClone III (HyClone), and penicillin-streptomycin. SGC1 cells were kindly supplied by Marie Piechocki (Wayne State University, Detroit, MI) and maintained at 37°C in 5% CO_2 in Dulbecco modified essential medium supplemented with 10% feta bovine serum (HyClone) and penicillin-streptomycin. To generate stable M33 expressing and control cell lines pTRE2Hyg-M33FLAG(WT) and pTRE2Hyg were transfected into HEK TET-OFF cells and selected in the presence of 200 μg of hygromycin/ml and 100 ng of doxycycline/ml. After the establishment of stable lines, the control and M33 cells were routinely cultured in the absence of doxycycline to allow for maximal expression of the M33 protein.

Retroviral production and transduction. M33FLAG(WT) and M33FLAG(R131A) cDNAs were blunt cloned into the HpaI site within the MigR1 retroviral vector and retrovirus was produced as described before (66). MigR1 is a bicistronic retroviral vector containing a multiple cloning site upsteam of an internal ribosome entry site, followed by the cDNA encoding enhanced green fluorescent protein (57). For transduction of SGC1 cells, 10^5 cells were plated in 12-well plates and 24 h later appropriate amounts of MigR1, MigR1-M33FLAG(WT), or MigR1-M33FLAG(R131A) supernatants were added to the media. At 48 h after transduction, cells were assayed by fluorescence-activated cell sorting as described previously (66).

Luciferase assays. For CREB reporter assays, HEK293 cells were transfected at 40 to 50% confluence in 100-mm dishes with 0.2 μg of pFA2-CREB, 0.5 μg of pFR-Luc, and 0.5 μg of pRL-CMV as an internal control. For NF-κB reporter assays, cells were transfected with 0.5 μg of 3X MHC-Luc and 0.5 μg of pRL-CMV as an internal control. At 24 h posttransfection, cells were split into collagen-coated 12-well plates and assayed the following day with the dual-luciferase reporter assay system (Promega) according to the manufacturer's protocol. Luciferase data were normalized to the *Renilla* luciferase activity and are presented as relative light units. For PKC depletion experiments, cells were treated overnight with 0.2 or 1.0 μM PMA prior to initiating the experiment. Western blots were performed to ensure depletion of PKCs throughout the duration of the experiment.

Immunoprecipitations and immunoblotting. For immunoprecipitation of M33FLAG(WT) and M33FLAG(R131A), cell lysates were prepared in 1.0 ml of NP-40 lysis buffer (50 mM HEPES, 0.5% Nonidet P-40, 250 mM NaCl, 10% glycerol, 2 mM EDTA, 1 mM phenylmethylsulfonyl fluoride, 2.5 μg of aprotinin/ml, 5.0 μg of leupeptin/ml, 100 μM sodium orthovanadate, and 1 mM sodium

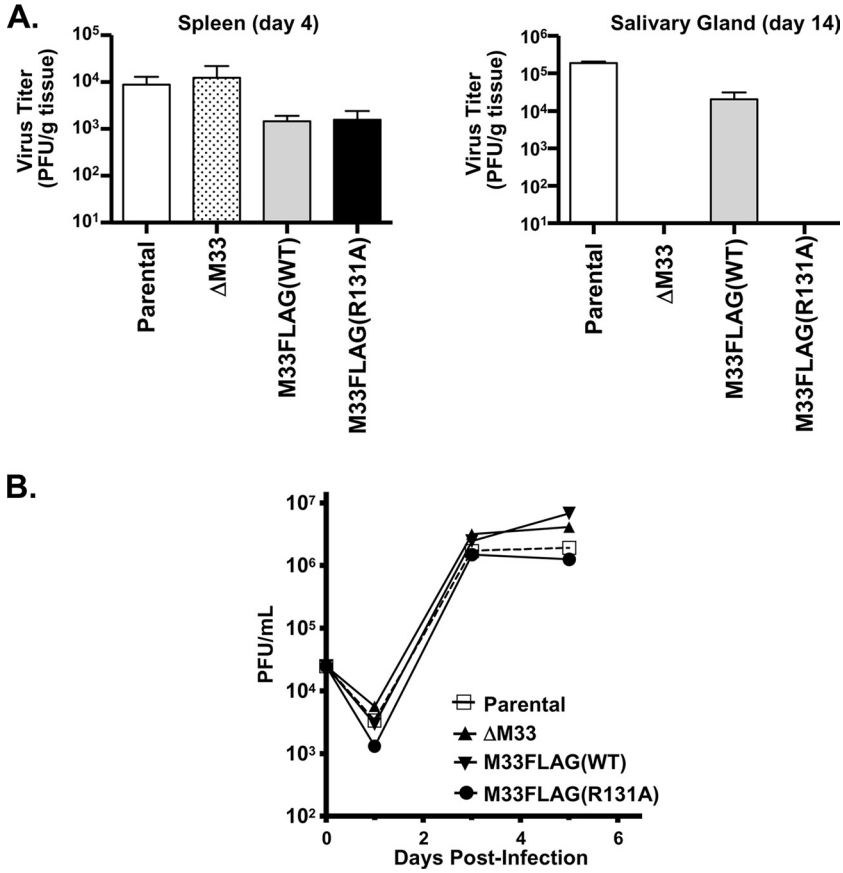

FIG. 1. M33FLAG(R131A) recombinant virus fails to persist in the salivary glands. (A) Female BALB/c Mice were infected intraperitoneally with 5×10^5 PFU of K181 BAC-derived parental, ΔM33, M33FLAG(WT), or M33FLAG(R131A) viruses. Groups of three mice were sacrificed on day 4 or day 14 postinfection, and their spleens and salivary glands were harvested. Tissues were homogenized, and virus titers were assessed by plaque assay on NIH 3T3 cells. Virus titers from spleens isolated at 4 days postinfection (left panel) or from salivary glands isolated at 14 days postinfection (right panel) are depicted graphically. (B) The ability of each of the BAC-derived viruses to replicate in salivary epithelial cells was also assessed in the salivary gland cell line SGC-1. Multistep growth curves were performed by infecting subconfluent SGC-1 cells at a multiplicity of infection of 0.1. Samples of tissue culture supernatant were taken at days 1, 3, and 5 postinfection, and virus titers were determined by plaque assay. The data represent the means of three independent experiments.

fluoride). Lysates were then incubated with 30 μl of anti-Flag M2-agarose beads (Sigma) and tumbled for 3 h at 4°C. Immunoprecipitated complexes were washed with NP-40 lysis buffer, solubilized in 3X Laemmli buffer, subjected to sodium dodecyl sulfate-polyacrylamide gel electrophoresis and transferred to nitrocellulose membranes. For direct immunoblotting (without an immunoprecipitation step), cell lysates were prepared directly in 3× Laemmli sample buffer (p38) or NP-40 lysis buffer (FLAG, VASP, PKCs, M44, and β-actin) prior to dilution in 3× sample buffer. Lysates were sonicated briefly, boiled for 5 min, separated by sodium dodecyl sulfate-polyacrylamide gel electrophoresis, and transferred to nitrocellulose. Nitrocellulose filters were then probed with the following antibodies; anti-VASP (Santa Cruz Biotechnology), anti-phospho-p38 (Thr180/Tyr182), anti-total p38 (Cell Signaling Technology), anti-FLAG (OctA-probe; Santa Cruz Biotechnology), anti-M44 (John Shanley, University of Connecticut), and anti-β-actin (James Lessard, Cincinnati Children's Hospital Medical Center). For all blots, incubation in appropriate horseradish peroxidase-conjugated anti-rabbit or anti-mouse immunoglobulin G (IgG) secondary antibodies (Amersham) and enhanced chemiluminescence were used for detection and visualization, respectively.

Inositol phosphate accumulation assays. Measurement of inositol phosphate accumulation as a readout of PLC-β activity was performed as previously described (66). The data are from at least three independent experiments performed in duplicate, and the inositol phosphate accumulation is presented as the percent conversion of total incorporated [^{3}H]myoinositol.

Measurement of intracellular calcium. At 24 h posttransfection, HEK293 cells were split into 96-well clear flat-bottom plates. The following day, the cells were labeled for 1 h with the Fluo-4 NW calcium assay dye according to the manufacturer's protocol (Molecular Probes). Free intracellular calcium was measured by using a FlexStationII (Molecular Devices). Cells were then lysed in 1% NP-40 for 20 min, and the total intracellular calcium was measured. Data from three independent experiments performed in quadruplicate are presented as the free intracellular calcium concentration divided by the total intracellular calcium concentration.

Virus reconstitution and growth curves. For virus reconstitution, NIH 3T3 cells (2×10^5 cells per six-well plate) were transfected with 1.0 to 3.0 μg of purified MCMV bacterial artificial chromosome (BAC) DNA (K181 strain) using *Trans*IT-LT1 transfection reagent according to the manufacturer's protocol. Infectious virus was harvested upon visible plaque formation (approximately 3 to 5 days posttransfection) and used to create virus stocks. Virus titers of stocks and tissue homogenates were determined by plaque assay on NIH 3T3 cells as previously described (13). For MCMV growth curves, viruses were used to infect cells at a multiplicity of infection of 0.1 (SGC1 cells) or 0.01 (NIH 3T3 cells), and the supernatant was harvested once a day for the following 7 days. Virus titers were determined as described above.

Mice and recombinant virus infection. Pathogen-free 6- to 7-week-old female BALB/c mice were purchased from Harlan Sprague-Dawley (Indianapolis, IN). A total of six mice per virus were infected intraperitoneally with 5×10^5 PFU, and spleens and salivary glands were harvested at 4 and 14 days postinfection, respectively. Virus titers were determined from homogenized tissues by plaque assay as described above and are expressed as PFU/g tissue.

Statistical analysis. GraphPad Prism software was used to perform paired Student *t* tests on all luciferase and p38 phosphorylation assays. All experiments were performed at least three independent times.

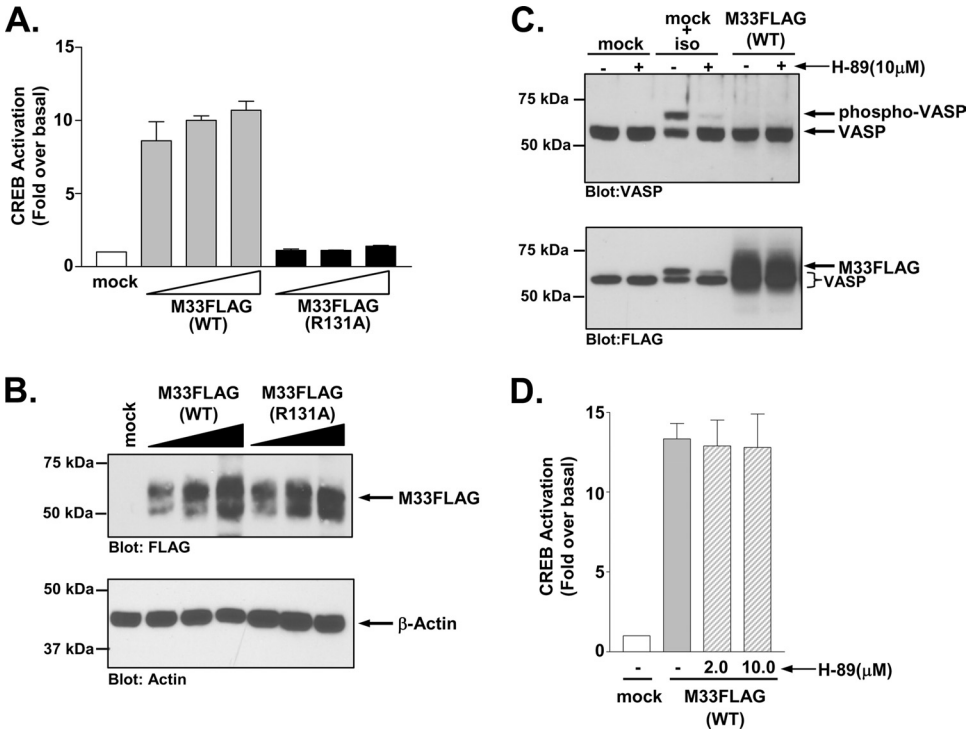

FIG. 2. M33 activates CREB independent of G_s coupling. (A) HEK293 cells were transiently transfected with empty vector (mock) or 50, 100, or 250 ng of M33FLAG(WT) or M33FLAG(R131A), and CREB-driven luciferase transcription was measured and normalized to *Renilla* luciferase. The data represent the means ± the standard errors (SE) of four independent experiments performed in duplicate. (B) The expression of M33FLAG(WT) and M33-FLAG(R131A) in similarly transfected HEK293 cells was assessed by Western blotting. (C) PKA activity, as assessed by the phosphorylation status of the PKA substrate VASP, was assessed by Western blotting in HEK293 cells stably transfected with empty vector (mock) or M33 (M33FLAG). Cells were also transfected with FLAG-VASP. Control cells (mock) unstimulated or stimulated with the β-adrenergic agonist isoproterenol (1 μM for 5 min) with or without pretreatment with the PKA inhibitor H-89 were included to validate the sensitivity and specificity of the assay. The phosphorylation status of VASP was assessed by Western blotting with an anti-VASP polyclonal antibody (upper panel). Expression of M33FLAG was confirmed by Western blotting with an anti-FLAG polyclonal antibody (lower panel). Note that the bands in the non-M33 transfected cells represent phosphorylated or nonphosphorylated VASP which, like M33, is also FLAG tagged. The immunoblots shown are representative of at least four independent experiments. (D) HEK293 cells were transiently transfected with empty vector (mock) or M33FLAG(WT) (250 ng of each), and CREB-driven luciferase transcription normalized to *Renilla* luciferase was measured in the presence or absence of the PKA inhibitor H-89 (2.0 or 10 μM for 24 h). The data represent the means ± the SE of three independent experiments performed in duplicate.

RESULTS

M33 signaling is required for MCMV replication in the salivary glands of mice. Disrupting M33 function, either through deletion of M33 or mutation of the M33 "DRY" signaling motif (R131Q), has no effect on MCMV replication in vitro but severely attenuates MCMV growth within the salivary gland in vivo (18, 21). The M33(R131Q) mutant was defective in PLC-β, CREB, and NFAT signaling; however, the effects of this mutation on other M33-stimulated signaling pathways, including p38 and NF-κB, were not assessed (18). Earlier work from our lab demonstrated that a similar mutant, M33(R131A), failed to stimulate GDP to GTP conversion on $G\alpha_{q/11}$ subunits and thus failed to activate $G_{q/11}$ signaling pathways (66). Prior to initiating mechanistic studies on the downstream signaling pathways activated by M33, we wanted to assess the phenotype of a MCMV mutant virus expressing the M33(R131A) mutant protein in vivo. We used recombinant DNA techniques to generate a MCMV (K181 strain) mutant with the entire M33 open reading frame (ORF) (ΔM33) deleted or MCMV mutants expressing either the M33FLAG (WT) or M33FLAG(R131A) mutant (see Fig. S1 in the supplemental material) (61). Using this strategy, the M33FLAG (WT) and M33FLAG(R131A) viruses represent "rescues" of the ΔM33 virus.

To assess MCMV replication in vivo, mice were infected with parental MCMV (K181 strain) or with the ΔM33, M33FLAG(WT), or M33FLAG(R131A) recombinant viruses. Virus titers from spleen and salivary glands were determined on days 4 and 14 postinfection, respectively, and are expressed as PFU/g (organ weight). High virus titers are detectable in the spleen at 4 days postinfection for the ΔM33, M33FLAG(WT), and M33FLAG(R131A) viruses and are comparable to those of the parental virus (Fig. 1, left panel). However, pronounced differences among virus titers were observed in the salivary glands at 14 days postinfection; parental and M33FLAG(WT) viruses replicate to high titers, whereas no recoverable virus was detected with the ΔM33 or M33FLAG(R131A) viruses (Fig. 1, right panel). These data are in support of previous findings (18, 21) and demonstrate that the M33 R131A mutation also inhibits the ability of M33 to enable MCMV replica-

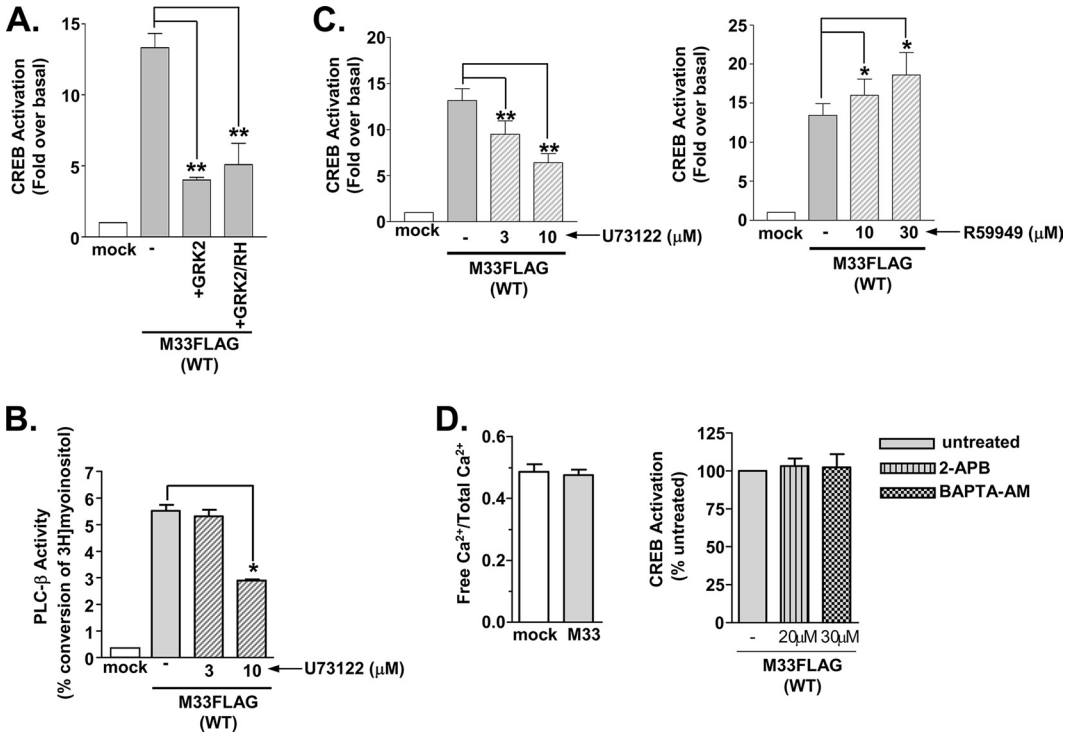

FIG. 3. M33-induced CREB activation occurs through the $G_{q/11}$/PLC-β pathway. (A) HEK293 cells were transiently transfected with empty vector (mock) or M33FLAG(WT) (250 ng) with or without GRK2 (250 ng) or the $G\alpha_{q/11}$-binding domain of GRK2 (GRK2/RH) (250 ng), and CREB-driven luciferase transcription was measured and normalized to *Renilla* luciferase. The data represent the means ± the SE of three independent experiments performed in duplicate. (B) HEK293 cells were transiently transfected with empty vector (mock) or M33FLAG(WT) (1.25 μg), and accumulated inositol phosphates were measured. M33-expressing cells were left untreated or treated with the PLC-β inhibitor U73122 (3 and 10 μM) for 24 h prior to assay. The data represent the means ± the SE of three independent experiments performed in duplicate. (C) CREB-driven luciferase activity normalized to *Renilla* luciferase was measured in HEK293 cells transiently transfected with M33FLAG(WT) (250 ng) untreated or treated with the PLC-β inhibitor U73122 (3 and 10 μM for 24 h, left panel) or the diacyglycerol kinase inhibitor R59949 (10 and 30 μM for 24 h, right panel). The data represent the means ± the SE of five independent experiments performed in duplicate. (D) Cells transiently transfected with empty vector or M33 (1.25 μg) were assessed for intracellular Ca^{2+} levels using Fluo-4 NW (left panel). CREB-driven luciferase activity normalized to *Renilla* luciferase was measured in HEK293 cells transiently transfected with M33FLAG(WT) (250 ng) untreated or treated with the IP_3 channel inhibitor 2-APB (20 μM for 24 h) or the calcium chelator BAPTA-AM (30 μM for 24 h, right panel). The data represent the means ± the SE of three independent experiments performed in duplicate. *, $P \leq 0.05$; **, $P \leq 0.005$.

tion within the salivary gland in vivo. Because the ΔM33 and M33FLAG(R131A) viruses failed to replicate to detectable levels in the salivary gland in vivo, we next sought to determine whether the loss of M33 signaling activity led to an inherent inability of MCMV to replicate in salivary epithelial cells (19, 58). Multistep growth curves determined in vitro in the salivary epithelial cell line SGC1 demonstrate that the ΔM33, M33FLAG(WT), and M33FLAG(R131A) viruses replicate to levels similar to those of wild-type MCMV (Fig. 1B). This result suggests that the in vivo defect exhibited by M33 signaling defective viruses is not due to an inability to replicate in salivary epithelial cells and could be the result of a failure to regulate immune responses in this particular tissue.

Correct generation of each MCMV recombinant was assessed by PCR analysis and EcoRI digestion and was confirmed by DNA sequencing (data not shown; but see Fig. S1 and S2 in the supplemental material). To ensure that the R131A mutation does not effect protein expression or stability, NIH 3T3 cells were infected with each virus and M33 expression was analyzed by immunoprecipitation and Western blotting. M33FLAG(WT) and M33FLAG(R131A) are similarly expressed at 24 h postinfection (although upon longer exposure, the expression of both wild-type and R131A M33 could be detected as early as 12 h) with expression levels increasing up to 72 h (see Fig. S3A in the supplemental material). Multistep growth curves show that ΔM33, M33FLAG(WT), and M33FLAG(R131A) display no inherent growth defects in fibroblasts in vitro similar to the experiments in SGC1 cells (see Fig. S3B in the supplemental material).

M33 stimulation of CREB is dependent on the activation of a $G_{q/11}$/PLC-β signaling pathway. Previous studies on the signaling pathways activated by the MCMV GPCR M33 and by the HCMV GPCRs US28 and UL33 demonstrated that all three receptors activate the cyclic AMP response-element binding (CREB) protein transcription factor (48, 75). CREB becomes activated when phosphorylated by upstream kinases such as PKA and PKC and functions in concert with other transcription factors to stimulate transcription of numerous genes involved in cell growth and survival (35). Under some circumstances, CREB has also been shown to play a critical role in the regulation of viral gene transcription (20, 41, 64). HCMV-UL33 activates CREB in a G_s/PKA-dependent manner, while HCMV-US28 appears to activate CREB through a $G_{q/11}$/PKC pathway. It remains unclear whether M33 functions

similarly to UL33 or US28 in this signaling capacity. To better define the mechanism by which M33 activates CREB, we first compared the ability of M33(WT) and M33(R131A) to stimulate CREB-driven luciferase transcription (Fig. 2A). Although M33(WT) displays dose-dependent CREB activation, M33(R131A) is unable to activate CREB, suggesting that M33-induced CREB activation is downstream of M33 signaling through heterotrimeric G proteins. These results were not due to differences in protein expression since similar levels of M33 and M33-R131A were detected by Western blotting (Fig. 2B).

To determine whether the M33, a $G_{q/11}$-coupled receptor, might induce CREB activation through promiscuous activation of G_s proteins, we tested whether M33 could induce phosphorylation of the PKA substrate vasodilator-stimulated phosphoprotein (VASP) (Fig. 2C) (30, 31). Stimulation of the G_s-coupled β_2-AR with isoproterenol induces high levels of phosphorylated VASP, as determined by an increased molecular mass of the VASP protein compared to unstimulated cells. This signaling activity is inhibited in the presence of 10 μM concentrations of the PKA inhibitor H-89, confirming the specificity of this assay as a readout for G_s/PKA activity (24, 55, 78). However, no VASP phosphorylation was detected in cells expressing M33, indicating that M33 did not couple to the G_s/PKA pathway (Fig. 2C, upper panel). Western blot analyses confirmed the expression of M33 (Fig. 2C, lower panel). We also measured M33-induced CREB activity in the presence of the PKA inhibitor H-89 and found that inhibition of PKA had no effect on M33-induced CREB activation, further suggesting that the M33 activation of CREB is not mediated by the G_s/PKA pathway (Fig. 2D).

Previous work from our lab has demonstrated that M33 directly activates heterotrimeric $G_{q/11}$ proteins and that GPCR kinase 2 (GRK2) inhibited this activity (66). In Fig. 3A, coexpression of GRK2 or a minigene construct expressing the regulator of G protein signaling homology (RH) domain of GRK2, which has been shown to bind specifically to and inhibit activated GTP-bound $G\alpha_{q/11}$ proteins, severely attenuated M33 activation of CREB (15, 63). These data corroborate the previous findings from our lab showing that the function of the GRK2/RH domain alone can inhibit M33 signaling and indicate that M33 activates CREB through a $G_{q/11}$-specific mechanism (66).

We next wanted to examine the effects of downstream components of the $G_{q/11}$ pathway, including PLC-β, IP_3/Ca^{2+}, and DAG on M33-stimulated CREB activity. In the presence of the PLC-β inhibitor U73122 (9, 77), M33 stimulation of IP_3 accumulation is significantly inhibited (Fig. 3B). Similar inhibition of PLC-β causes a significant decrease in M33 CREB activation (Fig. 3C, left panel). Interestingly, although a major effect of activation of the PLC-β/IP_3 pathway is the release of intracellular Ca^{2+}, no changes in intracellular Ca^{2+} levels could be detected in cells expressing M33 (Fig. 3D, left panel). These data suggest that although M33 potently activates the $G_{q/11}$ pathway and induces IP_3 in a constitutive, agonist-independent manner, the increased levels of IP_3 do not appear to activate ER calcium channels, leading to a demonstrable change in intracellular Ca^{2+} levels. To determine whether any low-level Ca^{2+} release mediated by IP_3 accumulation could contribute to M33-induced CREB signaling, intracellular Ca^{2+} activity

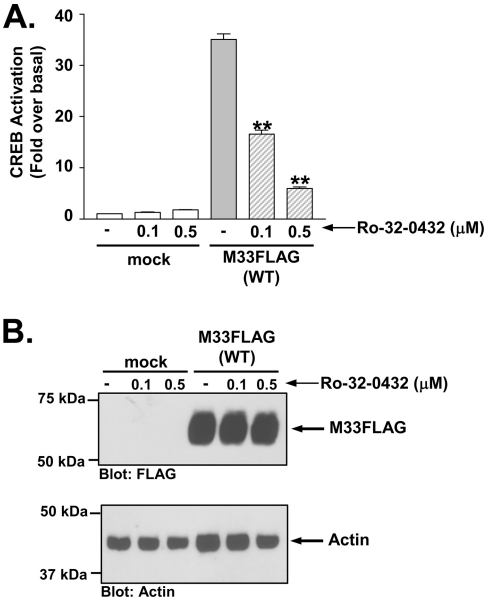

FIG. 4. M33-induced CREB activation is mediated by PKC. (A) HEK293 cells stably transfected with empty vector (mock) or M33FLAG were treated with the PKC inhibitor Ro-32-0432 (0.1 or 0.5 μM for 24 h) and CREB-driven luciferase activity was measured and normalized to *Renilla* luciferase. (B) Expression of M33FLAG was confirmed by Western blotting with an anti-FLAG polyclonal antibody. The data represent the means ± the SE of three independent experiments performed in duplicate. **, $P \leq 0.005$.

was inhibited by using the IP_3 receptor inhibitor 2-APB (20 μM) or the cell permeable Ca^{2+} chelator BAPTA-AM (30 μM) (60, 74, 76, 77). The same concentrations of 2-APB and BAPTA-AM were used in control experiments and demonstrated the ability to completely block the accumulation of free Ca^{2+} after stimulation of the lysophosphatidic acid receptor (data not shown). Neither 2-APB nor BAPTA-AM blocks CREB transcriptional activity in M33-expressing cells (Fig. 3D, right panel).

The second major effect of activation of Gq/PLC-β activation is the accumulation of DAG. To determine whether DAG accumulation plays a role in M33 activation of CREB, we inhibited DAG kinase to prevent DAG turnover, which leads to a stabilization of intracellular DAG levels. Treatment with the DAG kinase inhibitor R59949 (40, 73) significantly increases M33 stimulated CREB activity (Fig. 3C, right panel). Taken together, these results suggest that M33 stimulation of the $G_{q/11}$ pathway mediates CREB activation in a PLC-β/DAG-dependent manner. However, the downstream effects of PLC-β do not appear to involve the production of IP_3 or the release of Ca^{2+} from internal stores since inhibitors of these molecules had no affect on CREB activity.

M33 activates CREB in a PKC-dependent manner. Since PKC is a major downstream signal transducer of the $G_{q/11}$→PLC-β→DAG pathway, we wanted to determine whether it plays a prominent role in M33 activation of CREB. Although PKA is often thought of as the predominant kinase involved in CREB activation, studies have shown PKC can similarly phosphorylate and activate CREB (7, 29, 62). As demonstrated in Fig. 4A, pretreatment with the PKC inhibitor

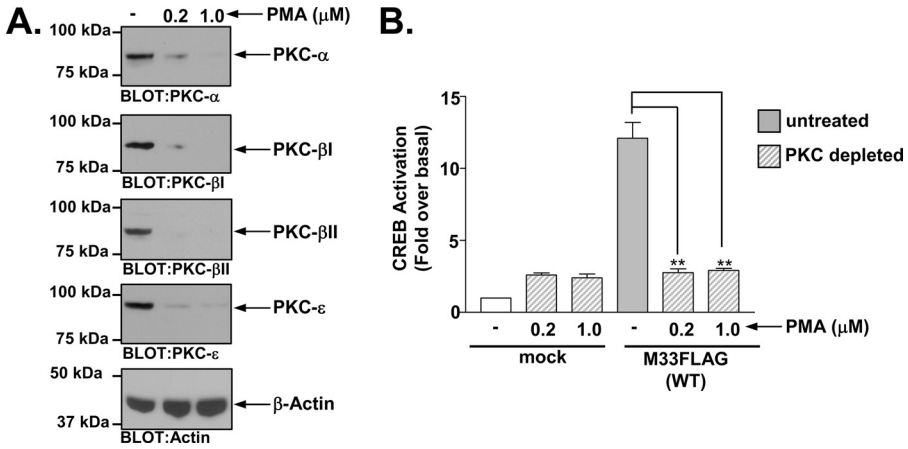

FIG. 5. M33-induced CREB activation is defective in PKC-depleted cells. (A) HEK293 cells were treated overnight with the phorbol ester PMA to deplete endogenous PKCs. HEK293 cells express several isoforms of PKC including PKC-α, PKC-β1, PKC-β2, and PKC-ε and Western blotting of cells treated with 0.2 or 1.0 μM PMA confirmed that these conditions resulted in >90% depletion of endogenous PKCs. (B) After depletion of endogenous PKCs, untreated or treated cells were transiently transfected with empty vector (mock) or M33FLAG(WT) (250 ng) and CREB-driven luciferase activity was measured and normalized to *Renilla* luciferase. The data represent the mean ± the SE of four independent experiments performed in duplicate. **, $P \leq 0.005$.

Ro-32-0432 at both 0.1 and 0.5 μM caused significant inhibition of M33-induced CREB activity (32, 78). Analyses of M33 expression in the presence of the PKC inhibitor Ro-32-0432 indicted that the PKC inhibitor had no effect on M33 expression (Fig. 4B). Note that the level of M33-induced CREB activity in Fig. 4 is somewhat higher than in earlier figures since we utilized a cell line stably expressing M33FLAG for this experiment. We also assessed the effects of two additional PKC inhibitors, bisindoylmaleimide I and Gö6976, on M33 induced CREB activation and observed a similar inhibition of M33 directed CREB activation (see Fig. S4 in the supplemental material). To garner additional evidence supporting a role for PKC in M33-induced CREB signaling, we treated cells overnight with phorbol myristate acetate (PMA) to deplete the cells of PKC (23, 49, 52, 72). HEK293 cells express at least four isoforms of PKC (α, β1, β2, and ε), which are all downregu-

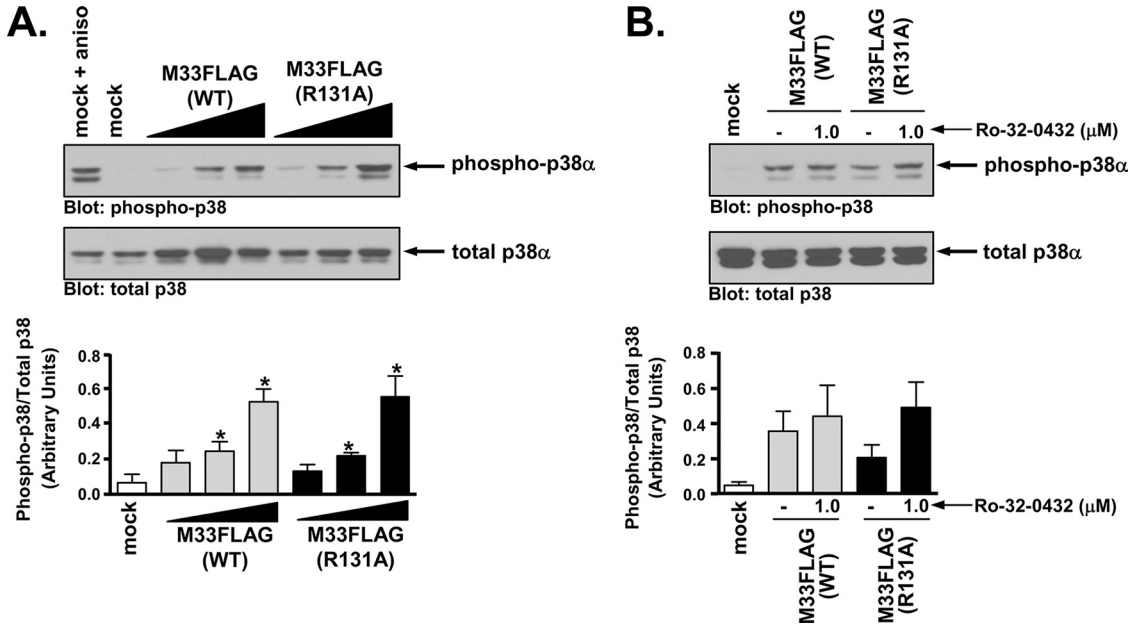

FIG. 6. M33 activates the MAPK p38 independent of $G_{q/11}$/PKC signaling. (A) HEK293 cells were cotransfected with M33FLAG(WT) or M33FLAG(R131A) (0.25, 0.50, and 1.25 μg) and FLAG-p38α (0.50 μg) and p38 phosphorylation was assessed by Western blotting (upper panel). As a positive control, mock-transfected cells were treated with the stress response activator anisomycin. The results are presented graphically and represent the means ± the SE of four independent experiments (lower panel). (B) Phosphorylated p38 levels in HEK293 cells expressing M33FLAG(WT) or M33FLAG(R131A) (1.25 μg of each) and FLAG-p38α (0.5 μg) were assessed in the presence or absence of the PKC inhibitor Ro-32-0432 (upper panel). The results are presented graphically and represent the means ± the SE of three independent experiments (lower panel). *, $P \leq 0.05$.

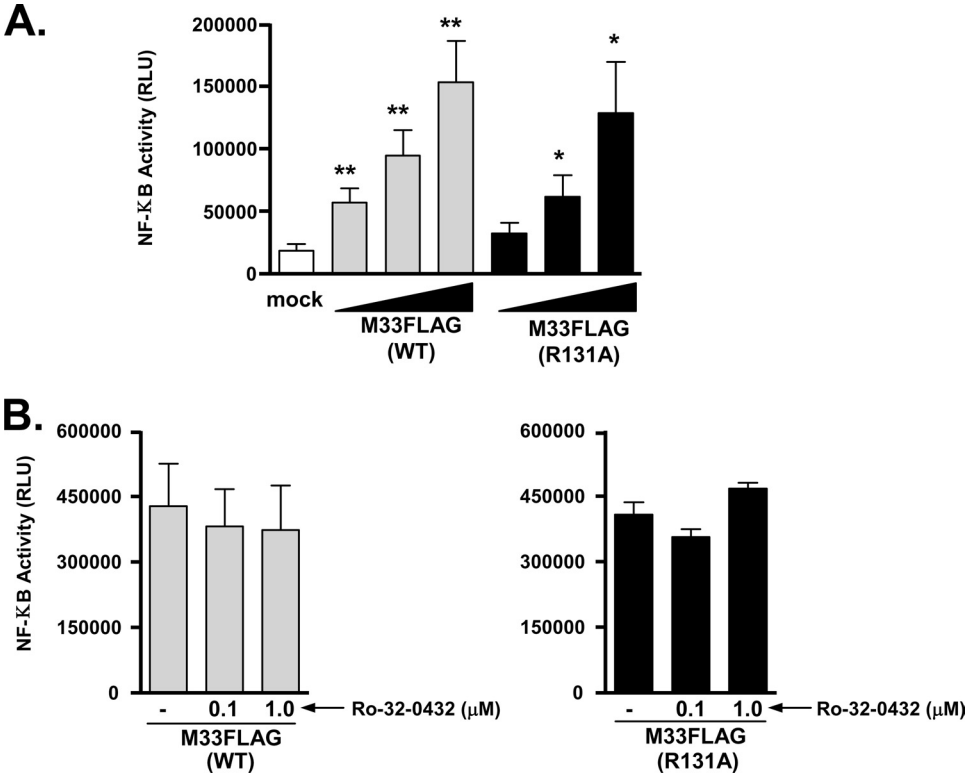

FIG. 7. Stimulation of NF-κB transcriptional activity by M33 is independent of $G_{q/11}$/PKC signaling. (A) HEK293 cells were transfected with empty pCDNA3 (mock) or increasing amounts of M33(WT) or M33(R131A) (10, 50, and 250 ng), and NF-κB-driven luciferase activity was measured and normalized to *Renilla* luciferase. The data represent the means ± the SE of five independent experiments performed in duplicate. (B) HEK293 cells transfected with M33(WT) or M33(R131A) (250 ng of each) were pretreated with the PKC inhibitor Ro-32-0432 (1.0 μM for 24 h) and NF-κB-driven luciferase activity was measured and normalized to *Renilla* luciferase. The data represent the means ± the SE of three independent experiments performed in duplicate. RLU, relative light units. *, $P \leq 0.05$; **, $P \leq 0.005$.

lated >90% using these conditions (Fig. 5A). In agreement with the PKC inhibitor data, this treatment completely abolished the ability of M33 to stimulate CREB (Fig. 5B). Taken together, these results provide strong evidence regarding the role of PKC in mediating M33 signaling to downstream transcription factors such as CREB. We do not know at this point which of the PKC isoforms are involved in this M33-induced signaling. However, since M33 does not appear to alter Ca^{2+} levels, the data suggest that the M33 signals through Ca^{2+}-independent PKC isoforms.

M33 activates p38 and NF-κB in a $G_{q/11}$- and PKC-independent manner. Since a series of genetic and pharmacological approaches indicated that M33 activation of CREB involves a $G_{q/11}$→PLC-β→PKC pathway, we next sought to determine whether this signaling axis was similarly responsible for other M33 signaling activities (75). The p38 MAPK has been reported to be involved in signaling via a number of viral GPCRs, including M33, US28, and the Kaposi's sarcoma-associated herpesvirus (KSHV) GPCR ORF74 (4, 48, 50, 75). The active form of p38 can be detected using phospho-specific antibodies recognizing Ser and Thr residues of p38 that are targets for phosphorylation by upstream kinases. To explore the mechanism by which M33 may stimulate p38 activity, we measured the phosphorylation state of p38α in the presence of increasing amounts of M33(WT) or the $G_{q/11}$ signaling-deficient mutant M33(R131A) (Fig. 6A). Both M33(WT) and M33(R131A) significantly induce p38 phosphorylation in a dose-dependent manner, suggesting that activation of $G_{q/11}$ signaling is not necessary for this effect. When assayed in the presence of 1.0 μM concentrations of the PKC inhibitor Ro-32-0432, a concentration at which M33-induced CREB activation was significantly inhibited, p38 phosphorylation was not blocked in either M33(WT)- or M33(R131A)-expressing cells (Fig. 6B). These data indicate that M33 induces p38 phosphorylation in a $G_{q/11}$/PKC-independent manner.

Studies have also shown that many of the viral GPCRs, including US28 and M33, can stimulate NF-κB transcriptional activity (16, 75). NF-κB can initiate innate antiviral immune responses by regulating the expression of a number of proinflammatory genes. However, KSHV and HCMV, among other viruses, have been shown to exploit NF-κB signaling to enhance viral pathogenesis. In the case of KSHV, activation of NF-κB prevents lytic reactivation to allow for the virus to remain latent in specific cell types, while HCMV-induced NF-κB stimulation plays a central role in the transendothelial migration of infected monocytes (27, 68). In Fig. 7A, we assessed NF-κB transcriptional activity in response to M33 $G_{q/11}$ signaling by using a luciferase reporter assay. Similar to p38, both M33(WT) and M33(R131A) activate NF-κB in a dose-dependent manner, suggesting NF-κB activation does not require $G_{q/11}$ signaling. In addition, NF-κB signaling is independent of PKC activation as both M33(WT) and M33(R131A)-

stimulated NF-κB levels are not inhibited in the presence of 0.1 or 1.0 μM concentrations of the PKC inhibitor Ro-32-0432 (Fig. 7B). Interestingly, similar studies with the rat CMV GPCR R33 indicated that R33 induces NF-κB in a G protein-dependent manner since a DRY motif mutant R33(R131A) failed to induce both G protein signaling and NF-κB (28). Taken together, these data suggest that the rodent CMV GPCR homologs of HCMV-UL33, namely, M33 and R33, appear to have evolved divergent mechanisms by which to activate NF-κB.

M33 activates PLC-β/IP$_3$ signaling in salivary epithelial cells. While the HEK293 cells provide an amenable system for studying the mechanism of M33-induced signaling, we sought to determine whether M33 signaled in a similar manner in a cell type that is relevant to the function of M33 in vivo. To this end, we assessed the ability of M33 to signal through the Gq/PLC-β pathway in the murine salivary epithelial cell line SGC1 (58). We utilized retrovirus transduction to introduce M33FLAG(WT) and M33FLAG(R131A) into the SGC1 cells and analyzed transduction efficiency by flow cytometry using the green fluorescent protein, which is coexpressed from the retrovirus (data not shown). SGC1 cells expressing M33FLAG (WT) exhibit a robust increase in PLC-β signaling activity, as assessed by measuring the production of total inositol phosphates (Fig. 8A). Cells transduced with an empty retrovirus, or cells transduced with M33FLAG(R131A) exhibited no increase in PLC-β signaling activity, confirming that the increased signaling is to due to the presence of the constitutively active M33 protein. M33 expression was confirmed by Western blotting as shown in Fig. 8B. These experiments provide key evidence demonstrating that the constitutive signaling of M33 through the Gq/PLC-β pathway occurs within a biologically relevant cell type necessary for viral persistence within the host. Moreover, these data suggest that M33 is likely signaling through these same pathways within the salivary gland in vivo.

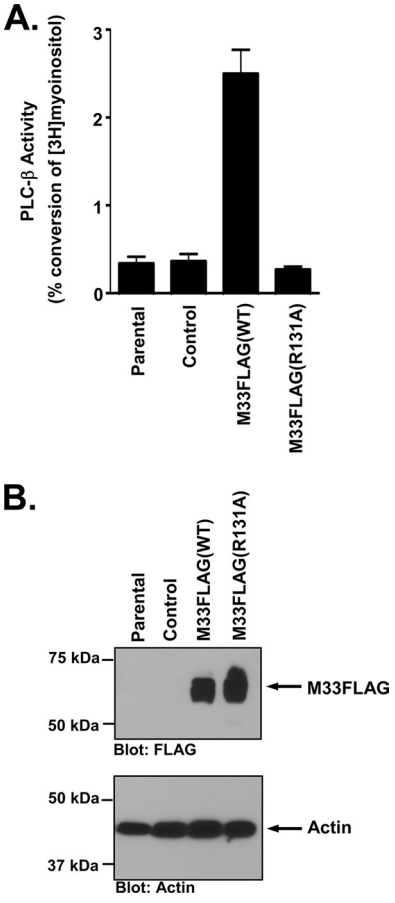

FIG. 8. M33 activates the $G_{q/11}$/PLC-β pathway in salivary epithelial cells. (A) SGC1 salivary epithelial cells were transduced with the retroviruses MIGR1, MIGR1-M33FLAG(WT), or MIGR1-M33FLAG(R131A). PLC-β activity was then measured in each cell line and is expressed as the percent conversion of input myoinositol into inositol phosphates. The data represent the means ± the SE of five independent experiments performed in duplicate. (B) Expression of M33FLAG and M33FLAG(R131A) in the transduced SGC1 cells was confirmed by Western blotting with an anti-FLAG polyclonal antibody (upper panel).

DISCUSSION

The results from the present study demonstrate that the MCMV-encoded GPCR M33 triggers the activation of intracellular signaling cascades via divergent mechanisms (Fig. 9). M33 activation of CREB is downstream of a classical $G_{q/11}$→PLC-β→PKC pathway, whereas p38 and NF-κB activity occur in a G protein/PKC-independent manner. Since the replication of the G protein signaling mutant M33(R131A) was determined to be severely blunted in vivo, we can not only begin to separate M33 signaling activities based on the requirement for G proteins but also determine the impact of these signaling activities on MCMV replication within important sites of MCMV persistence such as the salivary glands. Taken together, our data suggest that the G protein-independent signaling activity of M33 (i.e., phosphorylation of p38 and activation of NF-κB) is insufficient to support MCMV replication within sites of viral persistence while the G protein-dependent $G_{q/11}$→PLC-β→PKC pathway appears to be critical for M33 function in vivo.

For viral GPCRs, the published work from Case et al. first addressed the role of the DRY motif in terms of its affect on viral pathogenesis, namely, the impact on viral replication within an important immunological and epidemiological niche (18). While the M33(R131Q) mutant used in that study failed to initiate $G_{q/11}$ signaling and NFAT transcription, the possibility that the M33(R131Q) mutant would retain the ability to activate G protein-independent signaling pathways was not pursued. Our study is the first to demonstrate the modulation of intracellular signal transduction pathways from a viral GPCR in the absence of G protein signaling. Studies on a DRY mutant of the cellular angiotensin II type 1A GPCR, which fails to activate G proteins, demonstrated spatially and temporally distinct MAPK responses compared to signaling from wild-type receptors, suggesting potential differences in physiological responses may exist in vivo (1). Although not sufficient for MCMV replication in salivary glands, G protein-independent M33 signaling through p38 and/or NF-κB may play a supporting role in salivary gland replication or perhaps even a more central role in other aspects of M33 function. Identification of M33 mutants that retain G protein coupling

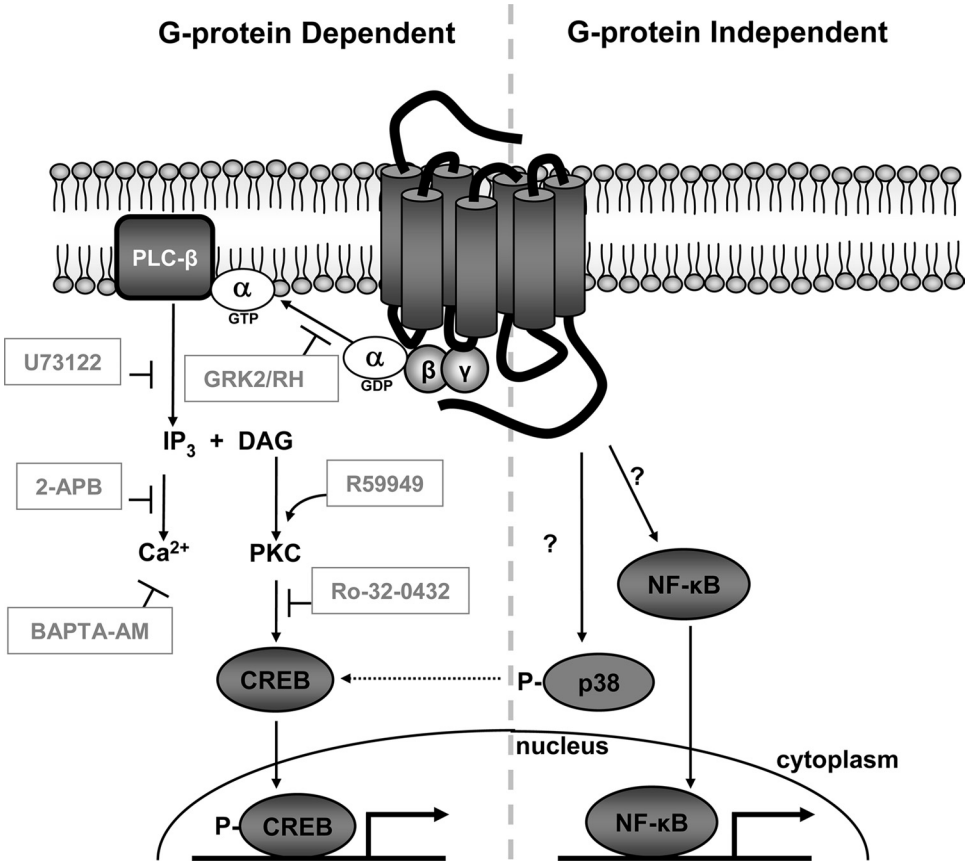

FIG. 9. G protein-dependent and G protein-independent signaling activities of M33. Use of pharmacological and genetic inhibitors at multiple steps along the $G_{q/11}$ signaling pathway reveals that CREB activation by the MCMV GPCR M33 is mediated by coupling to heterotrimeric $G_{q/11}$ proteins and PLC-β activity. Moreover, while not affected by IP_3 and Ca^{2+} levels, CREB activity is dependent on PKC activity and is augmented by increased levels of DAG. Conversely, M33 stimulation of p38 (which may partially contribute to M33-induced CREB activity) and NF-κB occurs in the absence of $G_{q/11}$ signaling through an as-yet-defined mechanism(s).

and yet fail to initiate p38 and/or NF-κB signaling will help to define the roles of these pathways during viral infection in vivo.

The G protein-independent mechanism by which M33 initiates p38 and NF-κB signaling remains unknown. A potential mechanism for M33-induced p38 phosphorylation could be the involvement of β-arrestin proteins, which bind to phosphorylated receptors during the desensitization process. Desensitized receptors have been shown to trigger second waves of G protein-independent signals through the scaffoldlike properties of β-arrestin, which allows for the formation of multicomponent signaling complexes (22, 51). Moreover, β-arrestin-dependent p38 activation has been shown for both cellular GPCRs and the HCMV GPCR US28 (10, 50, 71). In the case of US28, a truncation mutant lacking the β-arrestin binding domain in the carboxy terminus was defective in its ability to induce maximal levels of p38 phosphorylation compared to wild-type US28 (50). M33 has been shown to be phosphorylated by GRK2 and could thus be subject to β-arrestin-mediated desensitization as a mechanism to stimulate p38 signaling (66).

Based on our data, it appears that viral receptors such as M33, which constitutively activate PLC-β, do not necessarily alter the steady-state levels of intracellular Ca^{2+}. Thus, the effects of PLC-β appear to be primarily mediated by DAG and the Ca^{2+}-independent PKC isoforms but not by IP_3 and Ca^{2+}. It is possible that chronically high levels of IP_3 effectively desensitize the Ca^{2+} channels or that Ca^{2+} homeostasis is restored via alternative mechanisms. Currently, the direct impact of M33-stimulated PKC or CREB activation on MCMV pathogenesis in the salivary glands remains undetermined. MCMV infection of the submaxillary salivary gland occurs primarily within the acinar epithelial cells (33). These specialized cells form the apical lining of the salivary gland and constitute the major source of saliva secretion (54). Since CREB has also been shown to stimulate saliva secretion, M33 activation of $G_{q/11}$ and CREB within the salivary gland could potentiate the spread of MCMV to other cells within the salivary gland or even MCMV transmission from host to host (79). Enhanced PKC activity toward CREB (or other transcription factors) could also stimulate the expression of MCMV genes or cellular genes essential for viral growth in the salivary glands. Use of isoform-specific PKC inhibitors has revealed that novel PKC isoforms are necessary for MCMV IE1 and E1 protein expression and the establishment of MCMV infection in vitro (43). It remains possible that M33 could augment the effects of other MCMV gene products such as M50 and M53, which have been shown to enhance PKC phosphorylation and destabilize nuclear lamins, allowing for nuclear egress of nascent MCMV

capsids (53). Finally, PKC could be more broadly involved in the modulation of organ-specific immune response such as the induction of T-cell tolerance that has been observed in MCMV-infected salivary glands (34).

Using MCMV as a model for CMV GPCRs, we have defined the molecular pathway between $G_{q/11}$ coupling and CREB activation by the MCMV GPCR M33 and suggest that this pathway appears to be critical for MCMV replication in the salivary gland. Utilizing pharmacological or genetic inhibitors of PLC-β, PKC, or CREB may prove to prevent MCMV persistence within the salivary gland. The similarities observed between M33 and US28 signaling could suggest a comparable requirement for US28-dependent G protein signaling through PLC-β/PKC and CREB for efficient replication of HCMV in vivo. Perhaps inhibition of US28 signaling pathways could provide future therapeutic alternatives for treating persistent HCMV infection.

ACKNOWLEDGMENTS

We thank Syed Bilal Jilani and Ashley Reyer for help with establishing M33 cell lines and Nancy Sawtell, Richard Thompson, and Rhett Kovall for critical reading of the manuscript and for helpful discussions.

This study was supported by NIH grant AI058159 and by funds from the Cincinnati Microbial Pathogenesis Center (W.E.M.).

REFERENCES

1. **Ahn, S., S. K. Shenoy, H. Wei, and R. J. Lefkowitz.** 2004. Differential kinetic and spatial patterns of beta-arrestin and G protein-mediated ERK activation by the angiotensin II receptor. J. Biol. Chem. **279:**35518–35525.
2. **Alewijnse, A. E., H. Timmerman, E. H. Jacobs, M. J. Smit, E. Roovers, S. Cotecchia, and R. Leurs.** 2000. The effect of mutations in the DRY motif on the constitutive activity and structural instability of the histamine H(2) receptor. Mol. Pharmacol. **57:**890–898.
3. **Azzi, M., P. G. Charest, S. Angers, G. Rousseau, T. Kohout, M. Bouvier, and G. Pineyro.** 2003. Beta-arrestin-mediated activation of MAPK by inverse agonists reveals distinct active conformations for G protein-coupled receptors. Proc. Natl. Acad. Sci. USA **100:**11406–11411.
4. **Bais, C., B. Santomasso, O. Coso, L. Arvanitakis, E. G. Raaka, J. S. Gutkind, A. S. Asch, E. Cesarman, M. C. Gershengorn, and E. A. Mesri.** 1998. G-protein-coupled receptor of Kaposi's sarcoma-associated herpesvirus is a viral oncogene and angiogenesis activator. Nature **391:**86–89.
5. **Beisser, P. S., G. Grauls, C. A. Bruggeman, and C. Vink.** 1999. Deletion of the R78 G protein-coupled receptor gene from rat cytomegalovirus results in an attenuated, syncytium-inducing mutant strain. J. Virol. **73:**7218–7230.
6. **Beisser, P. S., C. Vink, J. G. Van Dam, G. Grauls, S. J. Vanherle, and C. A. Bruggeman.** 1998. The R33 G protein-coupled receptor gene of rat cytomegalovirus plays an essential role in the pathogenesis of viral infection. J. Virol. **72:**2352–2363.
7. **Blois, J. T., J. M. Mataraza, I. Mecklenbrauker, A. Tarakhovsky, and T. C. Chiles.** 2004. B-cell receptor-induced cAMP-response element-binding protein activation in B lymphocytes requires novel protein kinase Cδ. J. Biol. Chem. **279:**30123–30132.
8. **Boppana, S. B., R. F. Pass, W. J. Britt, S. Stagno, and C. A. Alford.** 1992. Symptomatic congenital cytomegalovirus infection: neonatal morbidity and mortality. Pediatr. Infect. Dis. J. **11:**93–99.
9. **Broad, L. M., F. J. Braun, J. P. Lievremont, G. S. Bird, T. Kurosaki, and J. W. Putney, Jr.** 2001. Role of the phospholipase C-inositol 1,4,5-trisphosphate pathway in calcium release-activated calcium current and capacitative calcium entry. J. Biol. Chem. **276:**15945–15952.
10. **Bruchas, M. R., T. A. Macey, J. D. Lowe, and C. Chavkin.** 2006. Kappa opioid receptor activation of p38 MAPK is GRK3- and arrestin-dependent in neurons and astrocytes. J. Biol. Chem. **281:**18081–18089.
11. **Bukowski, J. F., B. A. Woda, and R. M. Welsh.** 1984. Pathogenesis of murine cytomegalovirus infection in natural killer cell-depleted mice. J. Virol. **52:** 119–128.
12. **Burger, M., J. A. Burger, R. C. Hoch, Z. Oades, H. Takamori, and I. U. Schraufstatter.** 1999. Point mutation causing constitutive signaling of CXCR2 leads to transforming activity similar to Kaposi's sarcoma herpesvirus-G protein-coupled receptor. J. Immunol. **163:**2017–2022.
13. **Cardin, R. D., J. W. Brooks, S. R. Sarawar, and P. C. Doherty.** 1996. Progressive loss of $CD8^+$ T cell-mediated control of a gamma-herpesvirus in the absence of $CD4^+$ T cells. J. Exp. Med. **184:**863–871.
14. **Cardin, R. D., G. C. Schaefer, J. R. Allen, N. J. Davis-Poynter, and H. E. Farrell.** 2009. The M33 chemokine receptor homolog of murine cytomegalovirus exhibits a differential tissue-specific role during in vivo replication and latency. J. Virol. doi:10.1128/JVI.00386-09.
15. **Carman, C. V., J. L. Parent, P. W. Day, A. N. Pronin, P. M. Sternweis, P. B. Wedegaertner, A. G. Gilman, J. L. Benovic, and T. Kozasa.** 1999. Selective regulation of Gα(q/11) by an RGS domain in the G protein-coupled receptor kinase, GRK2. J. Biol. Chem. **274:**34483–34492.
16. **Casarosa, P., R. A. Bakker, D. Verzijl, M. Navis, H. Timmerman, R. Leurs, and M. J. Smit.** 2001. Constitutive signaling of the human cytomegalovirus-encoded chemokine receptor US28. J. Biol. Chem. **276:**1133–1137.
17. **Casarosa, P., Y. K. Gruijthuijsen, D. Michel, P. S. Beisser, J. Holl, C. P. Fitzsimons, D. Verzijl, C. A. Bruggeman, T. Mertens, R. Leurs, C. Vink, and M. J. Smit.** 2003. Constitutive signaling of the human cytomegalovirus-encoded receptor UL33 differs from that of its rat cytomegalovirus homolog R33 by promiscuous activation of G proteins of the Gq, Gi, and Gs classes. J. Biol. Chem. **278:**50010–50023.
18. **Case, R., E. Sharp, T. Benned-Jensen, M. M. Rosenkilde, N. Davis-Poynter, and H. E. Farrell.** 2008. Functional analysis of the murine cytomegalovirus chemokine receptor homologue M33: ablation of constitutive signaling is associated with an attenuated phenotype in vivo. J. Virol. **82:**1884–1898.
19. **Cavanaugh, V. J., D. H. Raulet, and A. E. Campbell.** 2007. Upregulation of CD94/NKG2A receptors and Qa-1b ligand during murine cytomegalovirus infection of salivary glands. J. Gen. Virol. **88:**1440–1445.
20. **Cougot, D., Y. Wu, S. Cairo, J. Caramel, C. A. Renard, L. Levy, M. A. Buendia, and C. Neuveut.** 2007. The hepatitis B virus X protein functionally interacts with CREB-binding protein/p300 in the regulation of CREB-mediated transcription. J. Biol. Chem. **282:**4277–4287.
21. **Davis-Poynter, N. J., D. M. Lynch, H. Vally, G. R. Shellam, W. D. Rawlinson, B. G. Barrell, and H. E. Farrell.** 1997. Identification and characterization of a G protein-coupled receptor homolog encoded by murine cytomegalovirus. J. Virol. **71:**1521–1529.
22. **DeWire, S. M., S. Ahn, R. J. Lefkowitz, and S. K. Shenoy.** 2007. Beta-arrestins and cell signaling. Annu. Rev. Physiol. **69:**483–510.
23. **Dwyer, J. R., N. Sever, M. Carlson, S. F. Nelson, P. A. Beachy, and F. Parhami.** 2007. Oxysterols are novel activators of the hedgehog signaling pathway in pluripotent mesenchymal cells. J. Biol. Chem. **282:**8959–8968.
24. **Farquhar, M. J., H. J. Harris, M. Diskar, S. Jones, C. J. Mee, S. U. Nielsen, C. L. Brimacombe, S. Molina, G. L. Toms, P. Maurel, J. Howl, F. W. Herberg, S. C. van Ijzendoorn, P. Balfe, and J. A. McKeating.** 2008. Protein kinase A-dependent step(s) in hepatitis C virus entry and infectivity. J. Virol. **82:**8797–8811.
25. **Flanagan, C. A.** 2005. A GPCR that is not "DRY". Mol. Pharmacol. **68:**1–3.
26. **Ge, L., Y. Ly, M. Hollenberg, and K. DeFea.** 2003. A beta-arrestin-dependent scaffold is associated with prolonged MAPK activation in pseudopodia during protease-activated receptor-2-induced chemotaxis. J. Biol. Chem. **278:** 34418–34426.
27. **Grossmann, C., and D. Ganem.** 2008. Effects of NFκB activation on KSHV latency and lytic reactivation are complex and context-dependent. Virology **375:**94–102.
28. **Gruijthuijsen, Y. K., E. V. Beuken, M. J. Smit, R. Leurs, C. A. Bruggeman, and C. Vink.** 2004. Mutational analysis of the R33-encoded G protein-coupled receptor of rat cytomegalovirus: identification of amino acid residues critical for cellular localization and ligand-independent signalling. J. Gen. Virol. **85:**897–909.
29. **Gubina, E., X. Luo, E. Kwon, K. Sakamoto, Y. F. Shi, and R. A. Mufson.** 2001. betac cytokine receptor-induced stimulation of cAMP response element binding protein phosphorylation requires protein kinase C in myeloid cells: a novel cytokine signal transduction cascade. J. Immunol. **167:**4303–4310.
30. **Halbrugge, M., and U. Walter.** 1990. Analysis, purification and properties of a 50,000-dalton membrane-associated phosphoprotein from human platelets. J. Chromatogr. **521:**335–343.
31. **Halbrugge, M., and U. Walter.** 1989. Purification of a vasodilator-regulated phosphoprotein from human platelets. Eur. J. Biochem. **185:**41–50.
32. **Haskew-Layton, R. E., A. A. Mongin, and H. K. Kimelberg.** 2005. Hydrogen peroxide potentiates volume-sensitive excitatory amino acid release via a mechanism involving Ca^{2+}/calmodulin-dependent protein kinase II. J. Biol. Chem. **280:**3548–3554.
33. **Henson, D., and A. J. Strano.** 1972. Mouse cytomegalovirus. Necrosis of infected and morphologically normal submaxillary gland acinar cells during termination of chronic infection. Am. J. Pathol. **68:**183–202.
34. **Humphreys, I. R., C. de Trez, A. Kinkade, C. A. Benedict, M. Croft, and C. F. Ware.** 2007. Cytomegalovirus exploits IL-10-mediated immune regulation in the salivary glands. J. Exp. Med. **204:**1217–1225.
35. **Johannessen, M., M. P. Delghandi, and U. Moens.** 2004. What turns CREB on? Cell Signal. **16:**1211–1227.
36. **Jonjic, S., W. Mutter, F. Weiland, M. J. Reddehase, and U. H. Koszinowski.** 1989. Site-restricted persistent cytomegalovirus infection after selective long-term depletion of $CD4^+$ T lymphocytes. J. Exp. Med. **169:**1199–1212.
37. **Jonjic, S., I. Pavic, P. Lucin, D. Rukavina, and U. H. Koszinowski.** 1990.

Efficacious control of cytomegalovirus infection after long-term depletion of $CD8^+$ T lymphocytes. J. Virol. **64:**5457–5464.
38. **Kedhar, S. R., and D. A. Jabs.** 2007. Cytomegalovirus retinitis in the era of highly active antiretroviral therapy. Herpes **14:**66–71.
39. **Khanna, R., and D. J. Diamond.** 2006. Human cytomegalovirus vaccine: time to look for alternative options. Trends Mol. Med. **12:**26–33.
40. **Kim, K. S., V. Rajagopal, C. Gonsalves, C. Johnson, and V. K. Kalra.** 2006. A novel role of hypoxia-inducible factor in cobalt chloride- and hypoxia-mediated expression of IL-8 chemokine in human endothelial cells. J. Immunol. **177:**7211–7224.
41. **Kim, Y. M., J. A. Ramirez, J. E. Mick, H. A. Giebler, J. P. Yan, and J. K. Nyborg.** 2007. Molecular characterization of the Tax-containing HTLV-1 enhancer complex reveals a prominent role for CREB phosphorylation in Tax transactivation. J. Biol. Chem. **282:**18750–18757.
42. **Krmpotic, A., I. Bubic, B. Polic, P. Lucin, and S. Jonjic.** 2003. Pathogenesis of murine cytomegalovirus infection. Microbes Infect. **5:**1263–1277.
43. **Kucic, N., H. Mahmutefendic, and P. Lucin.** 2005. Inhibition of protein kinases C prevents murine cytomegalovirus replication. J. Gen. Virol. **86:**2153–2161.
44. **Lagane, B., S. Ballet, T. Planchenault, K. Balabanian, E. Le Poul, C. Blanpain, Y. Percherancier, I. Staropoli, G. Vassart, M. Oppermann, M. Parmentier, and F. Bachelerie.** 2005. Mutation of the DRY motif reveals different structural requirements for the CC chemokine receptor 5-mediated signaling and receptor endocytosis. Mol. Pharmacol. **67:**1966–1976.
45. **Lee, B. J., U. H. Koszinowski, S. R. Sarawar, and H. Adler.** 2003. A gammaherpesvirus G protein-coupled receptor homologue is required for increased viral replication in response to chemokines and efficient reactivation from latency. J. Immunol. **170:**243–251.
46. **Lucin, P., I. Pavic, B. Polic, S. Jonjic, and U. H. Koszinowski.** 1992. Gamma interferon-dependent clearance of cytomegalovirus infection in salivary glands. J. Virol. **66:**1977–1984.
47. **Luttrell, L. M., F. L. Roudabush, E. W. Choy, W. E. Miller, M. E. Field, K. L. Pierce, and R. J. Lefkowitz.** 2001. Activation and targeting of extracellular signal-regulated kinases by beta-arrestin scaffolds. Proc. Natl. Acad. Sci. USA **98:**2449–2454.
48. **McLean, K. A., P. J. Holst, L. Martini, T. W. Schwartz, and M. M. Rosenkilde.** 2004. Similar activation of signal transduction pathways by the herpesvirus-encoded chemokine receptors US28 and ORF74. Virology **325:**241–251.
49. **Meszaros, J. G., R. Raphael, F. M. Lio, and L. L. Brunton.** 2000. Protein kinase C contributes to desensitization of ANG II signaling in adult rat cardiac fibroblasts. Am. J. Physiol. Cell Physiol. **279:**C1978–C1985.
50. **Miller, W. E., D. A. Houtz, C. D. Nelson, P. E. Kolattukudy, and R. J. Lefkowitz.** 2003. G-protein-coupled receptor (GPCR) kinase phosphorylation and beta-arrestin recruitment regulate the constitutive signaling activity of the human cytomegalovirus US28 GPCR. J. Biol. Chem. **278:**21663–21671.
51. **Miller, W. E., and R. J. Lefkowitz.** 2001. Expanding roles for beta-arrestins as scaffolds and adapters in GPCR signaling and trafficking. Curr. Opin. Cell Biol. **13:**139–145.
52. **Monick, M., J. Staber, K. Thomas, and G. Hunninghake.** 2001. Respiratory syncytial virus infection results in activation of multiple protein kinase C isoforms leading to activation of mitogen-activated protein kinase. J. Immunol. **166:**2681–2687.
53. **Muranyi, W., J. Haas, M. Wagner, G. Krohne, and U. H. Koszinowski.** 2002. Cytomegalovirus recruitment of cellular kinases to dissolve the nuclear lamina. Science **297:**854–857.
54. **Nauntofte, B.** 1992. Regulation of electrolyte and fluid secretion in salivary acinar cells. Am. J. Physiol. **263:**G823–G837.
55. **Obara, Y., H. Kurose, and N. Nakahata.** 2005. Thromboxane A2 promotes interleukin-6 biosynthesis mediated by an activation of cyclic AMP-response element-binding protein in 1321N1 human astrocytoma cells. Mol. Pharmacol. **68:**670–679.
56. **Oliveira, S. A., and T. E. Shenk.** 2001. Murine cytomegalovirus M78 protein, a G protein-coupled receptor homologue, is a constituent of the virion and facilitates accumulation of immediate-early viral mRNA. Proc. Natl. Acad. Sci. USA **98:**3237–3242.
57. **Pear, W. S., J. P. Miller, L. Xu, J. C. Pui, B. Soffer, R. C. Quackenbush, A. M. Pendergast, R. Bronson, J. C. Aster, M. L. Scott, and D. Baltimore.** 1998. Efficient and rapid induction of a chronic myelogenous leukemia-like myeloproliferative disease in mice receiving P210 bcr/abl-transduced bone marrow. Blood **92:**3780–3792.
58. **Piechocki, M. P., F. Lonardo, J. F. Ensley, T. Nguyen, H. Kim, and G. H. Yoo.** 2002. Anticancer activity of docetaxel in murine salivary gland carcinoma. Clin. Cancer Res. **8:**870–877.
59. **Pierce, K. L., R. T. Premont, and R. J. Lefkowitz.** 2002. Seven-transmembrane receptors. Nat. Rev. Mol. Cell. Biol. **3:**639–650.
60. **Poteser, M., I. Wakabayashi, C. Rosker, M. Teubl, R. Schindl, N. M. Soldatov, C. Romanin, and K. Groschner.** 2003. Crosstalk between voltage-independent Ca^{2+} channels and L-type Ca^{2+} channels in A7r5 vascular smooth muscle cells at elevated intracellular pH: evidence for functional coupling between L-type Ca^{2+} channels and a 2-APB-sensitive cation channel. Circ Res. **92:**888–896.
61. **Redwood, A. J., M. Messerle, N. L. Harvey, C. M. Hardy, U. H. Koszinowski, M. A. Lawson, and G. R. Shellam.** 2005. Use of a murine cytomegalovirus K181-derived bacterial artificial chromosome as a vaccine vector for immunocontraception. J. Virol. **79:**2998–3008.
62. **Rosethorne, E. M., S. R. Nahorski, and R. A. Challiss.** 2008. Regulation of cyclic AMP response-element binding-protein (CREB) by Gq/11-protein-coupled receptors in human SH-SY5Y neuroblastoma cells. Biochem. Pharmacol. **75:**942–955.
63. **Sallese, M., S. Mariggio, E. D'Urbano, L. Iacovelli, and A. De Blasi.** 2000. Selective regulation of Gq signaling by G protein-coupled receptor kinase 2: direct interaction of kinase N terminus with activated $G\alpha_q$. Mol. Pharmacol. **57:**826–831.
64. **Schwartz, R., B. Helmich, and D. H. Spector.** 1996. CREB and CREB-binding proteins play an important role in the IE2 86-kilodalton protein-mediated transactivation of the human cytomegalovirus 2.2-kilobase RNA promoter. J. Virol. **70:**6955–6966.
65. **Sherrill, J. D., and W. E. Miller.** 2008. Desensitization of herpesvirus-encoded G protein-coupled receptors. Life Sci. **82:**125–134.
66. **Sherrill, J. D., and W. E. Miller.** 2006. G protein-coupled receptor (GPCR) kinase 2 regulates agonist-independent Gq/11 signaling from the mouse cytomegalovirus GPCR M33. J. Biol. Chem. **281:**39796–39805.
67. **Smith, L. M., G. R. Shellam, and A. J. Redwood.** 2006. Genes of murine cytomegalovirus exist as a number of distinct genotypes. Virology **352:**450–465.
68. **Smith, M. S., E. R. Bivins-Smith, A. M. Tilley, G. L. Bentz, G. Chan, J. Minard, and A. D. Yurochko.** 2007. Roles of phosphatidylinositol 3-kinase and NF-κB in human cytomegalovirus-mediated monocyte diapedesis and adhesion: strategy for viral persistence. J. Virol. **81:**7683–7694.
69. **Streblow, D. N., S. L. Orloff, and J. A. Nelson.** 2007. Acceleration of allograft failure by cytomegalovirus. Curr. Opin. Immunol. **19:**577–582.
70. **Stropes, M. P., and W. E. Miller.** 2008. Functional analysis of human cytomegalovirus pUS28 mutants in infected cells. J. Gen. Virol. **89:**97–105.
71. **Sun, Y., Z. Cheng, L. Ma, and G. Pei.** 2002. Beta-arrestin2 is critically involved in CXCR4-mediated chemotaxis, and this is mediated by its enhancement of p38 MAPK activation. J. Biol. Chem. **277:**49212–49219.
72. **Taurin, S., K. Hogarth, N. Sandbo, D. M. Yau, and N. O. Dulin.** 2007. Gbetagamma-mediated prostacyclin production and cAMP-dependent protein kinase activation by endothelin-1 promotes vascular smooth muscle cell hypertrophy through inhibition of glycogen synthase kinase-3. J. Biol. Chem. **282:**19518–19525.
73. **Vega, R. B., B. C. Harrison, E. Meadows, C. R. Roberts, P. J. Papst, E. N. Olson, and T. A. McKinsey.** 2004. Protein kinases C and D mediate agonist-dependent cardiac hypertrophy through nuclear export of histone deacetylase 5. Mol. Cell. Biol. **24:**8374–8385.
74. **Vostal, J. G., and B. Shafer.** 1996. Thapsigargin-induced calcium influx in the absence of detectable tyrosine phosphorylation in human platelets. J. Biol. Chem. **271:**19524–19529.
75. **Waldhoer, M., T. N. Kledal, H. Farrell, and T. W. Schwartz.** 2002. Murine cytomegalovirus (CMV) M33 and human CMV US28 receptors exhibit similar constitutive signaling activities. J. Virol. **76:**8161–8168.
76. **Whitehead, J. P., J. C. Molero, S. Clark, S. Martin, G. Meneilly, and D. E. James.** 2001. The role of Ca^{2+} in insulin-stimulated glucose transport in 3T3-L1 cells. J. Biol. Chem. **276:**27816–27824.
77. **Wonerow, P., A. C. Pearce, D. J. Vaux, and S. P. Watson.** 2003. A critical role for phospholipase Cγ2 in αIIbβ3-mediated platelet spreading. J. Biol. Chem. **278:**37520–37529.
78. **Xie, Z., and G. M. Miller.** 2007. Trace amine-associated receptor 1 is a modulator of the dopamine transporter. J. Pharmacol. Exp. Ther. **321:**128–136.
79. **Yamada, K., H. Inoue, S. Kida, S. Masushige, T. Nishiyama, K. Mishima, and I. Saito.** 2006. Involvement of cAMP response element-binding protein activation in salivary secretion. Pathobiology **73:**1–7.